Physics Letters B 694 (2011) 301–309

Contents lists available at ScienceDirect

Physics Letters B

www.elsevier.com/locate/physletb

Precision measurement of the ratio $\mathrm{BR}(K_S \to \pi^+\pi^-e^+e^-)/\mathrm{BR}(K_L \to \pi^+\pi^-\pi^0_D)$

NA48/1 Collaboration

J.R. Batley [a], G.E. Kalmus [a,w], C. Lazzeroni [a,x], D.J. Munday [a], M. Patel [a,y], M.W. Slater [a,x], S.A. Wotton [a], R. Arcidiacono [b,s,t], G. Bocquet [b], A. Ceccucci [b], D. Cundy [b,z], N. Doble [b,n,p], V. Falaleev [b], L. Gatignon [b], A. Gonidec [b], P. Grafström [b], W. Kubischta [b], F. Marchetto [b,s], I. Mikulec [b,v], A. Norton [b,f,g], B. Panzer-Steindel [b], P. Rubin [b,aa,ab], H. Wahl [b,f,g], E. Goudzovski [c,x], P. Hristov [c,b], V. Kekelidze [c], V. Kozhuharov [c,ac], L. Litov [c], D. Madigozhin [c], N. Molokanova [c], Yu. Potrebenikov [c], S. Stoynev [c,k], A. Zinchenko [c], E. Monnier [d,ad], E.C. Swallow [d], R. Winston [d,ae], R. Sacco [e,af], A. Walker [e], W. Baldini [f,g], P. Dalpiaz [f,g], P.L. Frabetti [f,g,c], A. Gianoli [f,g], M. Martini [f,g], F. Petrucci [f,g], M. Savrié [f,g], M. Scarpa [f,g], M. Calvetti [h,i], G. Collazuol [h,i,n,o], E. Iacopini [h,i], G. Ruggiero [h,i,n,o], A. Bizzeti [i,ag], M. Lenti [i], M. Veltri [i,ah], M. Behler [j], K. Eppard [j], M. Eppard [j], A. Hirstius [j,b], K. Kleinknecht [j,b], U. Koch [j], P. Marouelli [j], L. Masetti [j], U. Moosbrugger [j], C. Morales Morales [j], A. Peters [j,b], R. Wanke [j], A. Winhart [j], A. Dabrowski [k,b], T. Fonseca Martin [k,ai], M. Szleper [k], M. Velasco [k], G. Anzivino [l,m], E. Imbergamo [l,m], G. Lamanna [l,m,b], P. Lubrano [l,m], A. Michetti [l,m], A. Nappi [l,m], M. Piccini [l,m], M. Valdata-Nappi [l,m], P. Cenci [m], M. Pepe [m], M.C. Petrucci [m], C. Cerri [n], R. Fantechi [n], I. Mannelli [n,o], F. Costantini [n,p], L. Fiorini [n,p,aj], S. Giudici [n,p], G. Pierazzini [n,p], M. Sozzi [n,p], C. Cheshkov [q,b,ak], J.B. Chèze [q], M. De Beer [q], P. Debu [q], G. Gouge [q], G. Marel [q], E. Mazzucato [q,*], B. Peyaud [q], B. Vallage [q], M. Holder [r], A. Maier [r,b], M. Ziolkowski [r], C. Biino [s], N. Cartiglia [s], M. Clemencic [s,t,b], S. Goy Lopez [s,t,al], E. Menichetti [s,t], N. Pastrone [s,t], W. Wislicki [u], H. Dibon [v], M. Jeitler [v], M. Markytan [v], G. Neuhofer [v], L. Widhalm [v]

[a] *Cavendish Laboratory, University of Cambridge, Cambridge, CB3 0HE, UK* [1]
[b] *CERN, CH-1211 Genève 23, Switzerland*
[c] *Joint Institute for Nuclear Research, Dubna 141980, Russian Federation*
[d] *The Enrico Fermi Institute, The University of Chicago, Chicago, IL 60126, USA*
[e] *Department of Physics and Astronomy, University of Edinburgh, JCMB King's Buildings, Mayfield Road, Edinburgh, EH9 3JZ, UK*
[f] *Dipartimento di Fisica dell'Università, I-44100 Ferrara, Italy*
[g] *Sezione dell'INFN di Ferrara, I-44100 Ferrara, Italy*
[h] *Dipartimento di Fisica dell'Università, I-50125 Firenze, Italy*
[i] *Sezione dell'INFN di Firenze, I-50125 Firenze, Italy*
[j] *Institut für Physik, Universität Mainz, D-55099 Mainz, Germany* [2]
[k] *Department of Physics and Astronomy, Northwestern University, Evanston, IL 60208, USA*
[l] *Dipartimento di Fisica dell'Università, I-06100 Perugia, Italy*
[m] *Sezione dell'INFN di Perugia, I-06100 Perugia, Italy*
[n] *Sezione dell'INFN di Pisa, I-56100 Pisa, Italy*
[o] *Scuola Normale Superiore, I-56100 Pisa, Italy*
[p] *Dipartimento di Fisica dell'Università, I-56100 Pisa, Italy*
[q] *DSM/IRFU – CEA Saclay, F-91191 Gif-sur-Yvette, France*
[r] *Fachbereich Physik, Universität Siegen, D-57068 Siegen, Germany* [3]
[s] *Sezione dell'INFN di Torino, I-10125 Torino, Italy*
[t] *Dipartimento di Fisica Sperimentale dell'Università, I-10125 Torino, Italy*
[u] *Soltan Institute for Nuclear Studies, Laboratory for High Energy Physics, PL-00-681 Warsaw, Poland* [4]
[v] *Österreichische Akademie der Wissenschaften, Institut für Hochenergiephysik, A-10560 Wien, Austria* [5]
[w] *Rutherford Appleton Laboratory, Chilton, Didcot, OX11 0QX, UK*
[x] *School of Physics and Astronomy, University of Birmingham, Birmingham B15 2TT, UK*
[y] *Imperial College London, Blackett Laboratory, Physics Department, Prince Consort Road, London SW7 2AZ, UK*
[z] *Istituto di Cosmogeofisica del CNR di Torino, I-10133 Torino, Italy*
[aa] *University of Richmond, Richmond, VA 23173, USA* [6]
[ab] *Department of Physics and Astronomy, George Mason University, Fairfax, VA 22030, USA*
[ac] *Faculty of Physics, University of Sofia "St. Kl. Ohridski", 1164 Sofia, Bulgaria*
[ad] *Centre de Physique des Particules de Marseille, IN2P3-CNRS, Université de la Méditerranée, Marseille, France*
[ae] *University of California, Merced, CA 95343, USA*

doi:10.1016/j.physletb.2010.10.008

[af] Department of Physics Queen Mary, University of London, Mile End Road, London E1 4NS, UK
[ag] Dipartimento di Fisica dell'Università di Modena e Reggio Emilia, I-41100, Modena, Italy
[ah] Istituto di Fisica, Università di Urbino, I-61029 Urbino, Italy
[ai] Laboratory for High Energy Physics, CH-3012 Bern, Switzerland
[aj] Institut de Fisica d'Altes Energies, Facultat Ciencias, Universitat Autonoma de Barcelona, E-08193 Bellaterra, Spain
[ak] Institut de Physique Nucléaire de Lyon, IN2P3-CNRS, Université Lyon I, F-69622 Villeurbanne, France
[al] Centro de Investigaciones Energeticas Medioambientales y Tecnologicas, E-28040 Madrid, Spain

ARTICLE INFO

Article history:
Received 18 August 2010
Received in revised form 27 September 2010
Accepted 6 October 2010
Available online 13 October 2010
Editor: W.-D. Schlatter

Keywords:
Neutral kaon radiative decay
Kaon rare decay
CP-violating asymmetry
Inner bremsstrahlung
Direct emission

ABSTRACT

The $K_S \to \pi^+\pi^-e^+e^-$ decay mode was investigated using the data collected in 2002 by the NA48/1 Collaboration. With about 23 k $K_S \to \pi^+\pi^-e^+e^-$ events and 59 k $K_L \to \pi^+\pi^-\pi^0_D$ normalization decays, the $K_S \to \pi^+\pi^-e^+e^-$ branching ratio relative to the $K_L \to \pi^+\pi^-\pi^0_D$ one was determined to be $\mathrm{BR}(K_S \to \pi^+\pi^-e^+e^-)/\mathrm{BR}(K_L \to \pi^+\pi^-\pi^0_D) = (3.28 \pm 0.06_{\mathrm{stat}} \pm 0.04_{\mathrm{syst}}) \times 10^{-2}$. This result was used to set the upper limit $|g_{E1}/g_{BR}| < 3.0$ at 90% CL on the presence, in the decay amplitude, of an E1 direct emission (g_{E1}) term relative to the dominant inner bremsstrahlung (g_{BR}) term. The CP-violating asymmetry $\mathcal{A}_\phi$ in the $\sin\phi\cos\phi$ distribution of $K_S \to \pi^+\pi^-e^+e^-$ events, where ϕ is the angle between the $\pi^+\pi^-$ and the e^+e^- decay planes in the kaon centre of mass, was found to be $\mathcal{A}_\phi = (-0.4 \pm 0.8)\%$, consistent with zero. These results are in good agreement with a description of the $K_S \to \pi^+\pi^-e^+e^-$ decay amplitude dominated by the CP-even inner bremsstrahlung process.

1. Introduction

The study of the radiative decay $K^0 \to \pi^+\pi^-\gamma^* \to \pi^+\pi^-e^+e^-$ provides an interesting ground for the investigation of CP non-invariance. It is well established now that the measurement of the angular correlation between the $\pi^+\pi^-$ and e^+e^- planes allows to test the presence of explicit CP-violating terms in the differential decay rate which are sensitive to the interference between amplitudes of opposite CP [1,2].

Such an interference term was observed in the $K_L \to \pi^+\pi^-e^+e^-$ decay mode by the KTeV [3,4] and NA48 [5] experiments through the measurement of a large asymmetry of about 14% in the $\sin\phi\cos\phi$ distribution of events, where ϕ is the angle between the $\pi^+\pi^-$ and the e^+e^- decay planes in the kaon centre of mass. This result is the consequence of the presence in the $K_L \to \pi^+\pi^-e^+e^-$ decay amplitude of two competing components: one from the CP-violating bremsstrahlung process in which the K_L decays into $\pi^+\pi^-$ with one of the pions radiating a virtual photon, the other from the CP-conserving direct emission process associated to the magnetic dipole M1 transition.

In the case of the short-lived neutral kaon, however, the decay amplitude into the $\pi^+\pi^-e^+e^-$ final state is expected to be largely dominated by the CP-even inner bremsstrahlung transition [6]. Therefore, no asymmetry should be observed. A departure from this prediction would reveal the existence of a sizeable CP-odd component in the decay amplitude.

In the approximation of a pure bremsstrahlung process, the amplitude of the $K_S \to \pi^+\pi^-e^+e^-$ decay can be written as [1,2]:

$$\mathcal{M}_{\mathrm{BR}} = e^2 g_{\mathrm{BR}} e^{i\delta_0(M_K^2)} \left[\frac{p_{+\mu}}{p_+\cdot k} - \frac{p_{-\mu}}{p_-\cdot k}\right] \frac{\bar{u}(k_-)\gamma^\mu v(k_+)}{k^2} \tag{1}$$

where e is the electric charge, p_+, p_-, k_+, k_- are the 4-momenta of the π^+, π^-, e^+, e^- particles, respectively, $k = k_+ + k_-$ and $\delta_0(M_K^2)$ is the $\pi\pi$ scattering phase in the $I = J = 0$ channel at the centre of mass energy equal to the kaon mass M_K. The g_{BR} parameter is related to the $K_S \to \pi^+\pi^-$ decay width by:

$$\Gamma(K_S \to \pi^+\pi^-) = \frac{g_{\mathrm{BR}}^2}{16\pi M_K}\left[1 - \frac{4M_\pi^2}{M_K^2}\right]^{1/2} \tag{2}$$

where M_π is the pion mass.

The first observation of the $K_S \to \pi^+\pi^-e^+e^-$ decay mode was obtained by NA48 using the data collected in 1998, concurrently with a run dedicated to the measurement of the $\mathrm{Re}(\varepsilon'/\varepsilon)$ parameter in neutral kaon decays. Based on a sample of 56 events, the branching ratio was measured to be $\mathrm{BR}(K_S \to \pi^+\pi^-e^+e^-) = (4.7 \pm 0.7_{\mathrm{stat}} \pm 0.4_{\mathrm{syst}}) \times 10^{-5}$ [7]. This result was improved later on by including the data collected in 1999 during the $\mathrm{Re}(\varepsilon'/\varepsilon)$ run and during a special 2-day test dedicated to the investigation of rare decays with an intense K_S beam [5]. The branching ratio obtained with the combined 1998–1999 statistics was $\mathrm{BR}(K_S \to \pi^+\pi^-e^+e^-) = (4.69 \pm 0.30) \times 10^{-5}$ and the corresponding asymmetry was found to be $\mathcal{A}_\phi = (-1.1 \pm 4.1)\%$. These measurements were based on a total sample of 678 candidates.

We report in this Letter the investigation of the $K_S \to \pi^+\pi^-e^+e^-$ decay with a significantly improved statistical sample using the NA48 experimental set-up and a high-intensity K_S beam. The $K_S \to \pi^+\pi^-e^+e^-$ branching ratio relative to the one of the normalization $K_L \to \pi^+\pi^-\pi^0_D$ decay mode as well as the $\mathcal{A}_\phi$ asymmetry parameter were determined. The data collected by this experiment allowed the precision of the existing measurements to be significantly improved by a statistics increase of more than a factor thirty.

* Corresponding author.
E-mail address: edoardo.mazzucato@cea.fr (E. Mazzucato).

[1] Funded by the UK Particle Physics and Astronomy Research Council.
[2] Funded by the German Federal Minister for Research and Technology (BMBF) under contract 7MZ18P(4)-TP2.
[3] Funded by the German Federal Minister for Research and Technology (BMBF) under contract 056SI74.
[4] Supported by the Committee for Scientific Research grants 5P03B10120, SPUB-M/CERN/P03/DZ210/2000 and SPB/CERN/P03/DZ146/2002.
[5] Funded by the Austrian Ministry for Traffic and Research under the contract GZ 616.360/2-IV GZ 616.363/2-VIII, and by the Fonds für Wissenschaft und Forschung FWF Nr. P08929-PHY.
[6] Supported in part by the US NSF under award #0140230.

2. Experimental setup

The data presented in this Letter were collected during 60 days in 2002 using the NA48 detector and a high-intensity neutral K_S beam at the CERN SPS [8]. A proton beam with a nominal momentum of 400 GeV/c and an average intensity of 4.8×10^{10} particles per pulse impinged on a Be target to produce secondary particles. The spill length was 4.8 s out of a 16.2 s cycle time. Charged particles were removed by a sweeping magnet and a 5.1 m long collimator which selected a beam of neutral particles at an angle of 4.2 mrad with respect to the proton beam.

Downstream of the collimator, the neutral beam and the decay products travelled in a 90 m long vacuum tank where most of the short-lived kaons (K_S), neutral hyperons (Λ^0, Σ^0), as well as a small fraction of long-lived neutral kaons (K_L) decayed. Undecayed particles like K_L, n and γ were directed towards a beam dump via a vacuum pipe that traversed all detector elements. On average, about 2×10^5 K_S per spill decayed in the fiducial volume downstream of the collimator with a mean energy of 120 GeV.

A magnetic spectrometer consisting of four drift chambers inside a helium-filled tank and a magnet with a horizontal transverse momentum kick of 265 MeV/c was located downstream of the vacuum tank which was terminated by a 0.3% X_0 thick *Kevlar* window. The space resolution obtained in a drift chamber was about 120 μm per projection and the momentum resolution could be parametrized as $\sigma_p/p = (0.48 \oplus 0.015p)\%$ with momentum p in GeV/c. This provided a resolution of 3 MeV/c^2 in the $\pi^+\pi^-$ invariant mass. The track time resolution was about 1.4 ns. A scintillator hodoscope was placed downstream of the spectrometer to provide accurate time information of charged particles ($\sigma_t \sim 250$ ps). It was made of two planes segmented in horizontal and vertical strips and arranged in four quadrants. The scintillator hodoscope was also used in the fast trigger logic.

The tracking detector was followed by a $27X_0$ deep liquid krypton calorimeter having a 2 cm × 2 cm cell transverse segmentation for the detection and measurement of electromagnetic showers. The achieved energy resolution could be parametrized as $\sigma_E/E = (3.2/\sqrt{E} \oplus 9.0/E \oplus 0.42)\%$ with E expressed in GeV. The transverse position resolution for a single photon of energy larger than 20 GeV was better than 1.3 mm and the obtained $\gamma\gamma$ invariant mass resolution for π^0 decays was about 1 MeV/c^2. The time resolution of the calorimeter for a single shower was better than 300 ps.

The electromagnetic calorimeter was followed by a hadron calorimeter and a muon detector. The fiducial volume of the experiment was determined by the spectrometer and LKr calorimeter acceptances together with an ensemble of seven rings of scintillation counters (AKL) used to veto activity outside this region.

3. The 4-track trigger

In order to select events compatible with decays into four charged particles, a specific Level 2 trigger (L2) that performed fast tracking of charged particles in the spectrometer was used [9]. It received signals from the earlier Level 1 trigger stage (L1) which required a minimum number of hits in the most upstream drift chamber and in the scintillator hodoscope, compatible with at least two tracks. The L1 condition required also no hit detected in the two most downstream AKL ring counters, a total energy seen in the electromagnetic and hadronic calorimeters greater than 30 GeV or at least 15 GeV measured in the LKr calorimeter. The output rate of the L1 stage was about 125 kHz. The measured efficiency of the L1 charged trigger for 4-track events of energy greater than 60 GeV was $99.8 \pm 0.1\%$.

The 4-track trigger used 300 MHz processors allowing complex events to be treated. It required at least three reconstructed space-points in the two drift chambers upstream of the magnet as well as in the last one, and a minimum of two compatible 2-track vertices within 3 m along the longitudinal kaon direction. No condition on the invariant mass of the selected 4-track candidates was imposed. The output rate of the 4-track trigger was about 500 Hz and represented 4% of the total Level 2 rate of the experiment. The dead time of the 4-track trigger logic was about 2%.

The 4-track trigger efficiency was measured from a sample of downscaled triggers that passed the L1 condition. It was found to be $(88.4 \pm 1.3)\%$ for $K_S \to \pi^+\pi^-e^+e^-$ decays and $(90.8 \pm 0.8)\%$ for the normalization $K_L \to \pi^+\pi^-\pi^0_D$ channel, where the quoted uncertainties are purely statistical. The main sources of trigger inefficiencies were attributed to wire inefficiencies, accidental activity and high-multiplicity events in the spectrometer. A small fraction (3%) of events was lost due to the maximum latency of 102.4 μs allocated to process the events. To study possible biases introduced by these event losses, about 10% of charged triggers which exceeded the available processing time were recorded. The analysis of these events showed that the trigger inefficiency between signal and normalization events was consistent within 0.5%.

A hardware failure which caused a time information mismatch between different drift chambers was found to affect about 8% of the recorded events. These well identified events were rejected from the final data sample as the corresponding 4-track efficiency was found to be significantly lower.

A total of 4.14×10^8 4-track triggers were thus selected for the offline analysis.

4. Event selection

The identification of $K_S \to \pi^+\pi^-e^+e^-$ candidates required four tracks reconstructed inside the fiducial volume of the NA48 detector. An outer radius cut of 120 cm and an 11 cm minimum radius cut around the centre of the beam pipe at each chamber position were imposed on particles entering the spectrometer. In addition, all four tracks were required to impinge on the electromagnetic calorimeter sufficiently far from the beam pipe and the outer edge (15 cm $< r_{LKr} <$ 120 cm) to ensure efficient electron identification with negligible energy losses. Tracks with an impact point closer than 2 cm to a dead calorimeter cell were rejected. For precise timing purposes, each track was required to have at least one associated hit in the scintillator hodoscope located in front of the LKr calorimeter. The averaged time of each of the six combinations of pairs of tracks was required to lie within 20 ns of the trigger time. Moreover, to reduce accidental activity, pairs of tracks were required to have consistent time measurements within 1.4 ns.

Electrons were identified by requiring an E/p value between 0.9 and 1.1 while tracks were designated as pions if they had $E/p < 0.8$ and no associated hit in coincidence, within 2 ns, in the muon counters. In order to suppress fake tracks due to accidental hits in the chambers, a χ^2 value smaller than 30 was required as a track quality cut. We required also that both the electron and pion pairs have two particles of opposite charge and that the reconstructed momentum be above 2 GeV/c for electron candidates, and above 10 GeV/c for pions.

A vertex made of four tracks passing the above cuts was formed if each of the six combinations of pairs of tracks had a closest distance of approach smaller than 10 cm and a reconstructed vertex located upstream of the *Kevlar* window ($z_{VTX} < 90$ m). The rejection of fake vertices made of two overlapping decays was obtained by imposing, as a vertex quality cut, a χ^2 value smaller than 50. The resolutions obtained on the transverse and longitudinal positions of the vertex are about 2 mm and 70 cm, respectively.

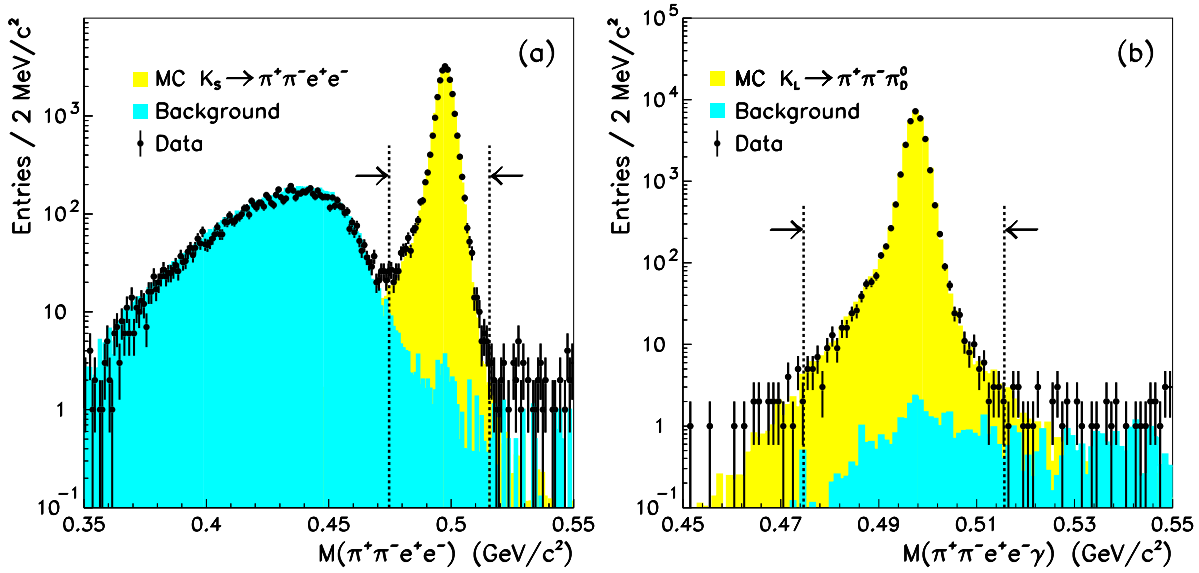

Fig. 1. Invariant $M_{\pi\pi ee}$ (a) and $M_{\pi\pi ee\gamma}$ (b) mass distributions for $K_S \to \pi^+\pi^-e^+e^-$ and $K_L \to \pi^+\pi^-\pi^0_D$ candidates, respectively, with the corresponding background contributions and Monte Carlo predictions. The arrows indicate the signal region.

The momentum vector of the 4-track event was extrapolated upstream to the exit face of the final collimator, where it was required to be contained within a radius of 2.5 cm around the K_S collimator hole. The angular resolution on the direction of the reconstructed kaon momentum vector was measured to be about 35 μrad (rms).

To remove events due to beam particles scattering in the collimators, we required the quantity $\vec{r}_{COG}$, defined as $\vec{r}_{COG} = \sum_i \vec{r}_i E_i / \sum_i E_i$, where E_i is the energy of the detected particle and $\vec{r}_i$ the corresponding transverse position vector at the liquid krypton calorimeter position z_{LKr}, to lie well inside the beam pipe. For a charged particle, the quantity $\vec{r}_i$ was obtained from the extrapolation to z_{LKr} of the upstream segment of the associated track. A radius cut of 7 cm was applied. This cut was chosen relatively wide compared to the K_S beam spot radius of 4.6 cm. It removed about 2% of signal events which originated mainly from beam scattering in the collimators. Moreover, $K_S \to \pi^+\pi^-e^+e^-$ candidates whose longitudinal vertex position was smaller than 7.5 m, that is, less than 1.5 m downstream of the exit face of the K_S collimator, were not considered. We demanded also that the square of the total transverse momentum $p_\perp^2$ of the observed decay products relative to the line of flight joining the centre of the K_S target to the parent kaon decay point be less than 1×10^{-2} GeV$^2/c^2$. The resolution obtained on $p_\perp^2$ is about 5×10^{-4} GeV$^2/c^2$ for $K_S \to \pi^+\pi^-e^+e^-$ decays. This condition, when applied after the cut on $\vec{r}_{COG}$, removed about 30% of the remaining events due to beam scattering in the collimators, while about 98% of good signal events were kept.

$K_S \to \pi^+\pi^-e^+e^-$ candidates were accepted if the kaon energy was comprised in the 60 to 160 GeV range. The minimum energy requirement is above the threshold value of 30 GeV set in the L1 trigger for the total energy measured in the calorimeters. To reduce background contributions from $\pi^+\pi^-e^+e^-$ final states from decays of K_L produced in the K_S target, the reconstructed kaon lifetime was required to be smaller than $7\tau_S$, where the origin was taken as the centre of the kaon production target.

Background events coming from $K_S \to \pi^+\pi^-\gamma$ decays followed by a photon conversion in the *Kevlar* window or in the first drift chamber were suppressed by imposing a 2 cm separation between the two electron tracks in the first drift chamber. This requirement also allowed the events originating from a $K_L \to \pi^+\pi^-\pi^0$ decay followed by the external conversion of one of the two decay photons of the π^0 to be rejected.

In order to reduce background contamination from accidental overlaps of $K_{L,S} \to \pi^+\pi^-$ decays with photon conversions in the collimators or in the detector material in front of the first chamber, events were eliminated if the reconstructed $\pi^+\pi^-$ invariant mass was found to lie within 15 MeV/c^2 of the neutral kaon mass. Moreover, the measured time of a pion pair was required to be compatible within 1.4 ns of the time measured for the lepton pair. Accidental background was further suppressed by rejecting events with an extra track measured in the spectrometer within 1.4 ns of the event time.

Possible background contributions from $\Xi^0 \to \Lambda\pi^0_D$ decays could be suppressed by removing events compatible with a $\Lambda \to p\pi$ decay. Four-track candidates with the two hadrons having a $p\pi$ invariant mass within 8 MeV/c^2 of the Λ mass value were eliminated.

A potential source of background to the $K_S \to \pi^+\pi^-e^+e^-$ channel originated from $K_L \to \pi^+\pi^-\pi^0_D$ decays when the photon from the π^0 Dalitz decay escaped detection. However, the acceptance of such events was very small owing to the larger decay length of the long-lived neutral kaon. In addition, because of the missing particle, the reconstructed mass was systematically below the kaon mass. To suppress this background contamination, we imposed to the remaining candidates the condition $-23 < M_{\pi\pi ee} - M_K < 18$ MeV/c^2. The latter cut was chosen asymmetrically with respect to the kaon mass in order to take into account the radiative tail observed at lower mass values.

The total number of $K_S \to \pi^+\pi^-e^+e^-$ candidates contained in the signal region amounted to 22 966. The $M_{\pi\pi ee}$ distribution of events obtained after all other selection criteria were applied is shown in Fig. 1(a).

The total background contamination in the $K_S \to \pi^+\pi^-e^+e^-$ sample, estimated using Monte Carlo simulations and data, was found to be 103.0 ± 10.2. The various contributions to the background are given in Table 1. The largest contribution originated from $K_L \to \pi^+\pi^-\pi^0$ decays (61%) followed by the decay of the neutral pion into a final state containing at least one e^+e^- pair. About 12% of the background contained $\pi^+\pi^-e^+e^-$ events from the decay of the K_L component in the beam and about 11% was due to accidental activity in the detectors. A fraction of unwanted

Table 1
Background to $K_S \to \pi^+\pi^-e^+e^-$.

Source	$N^{bkg}_{\pi\pi ee}$
Collimator scattering	16.2 ± 5.7
Accidental activity	11.0 ± 3.2
$K_L \to \pi^+\pi^-e^+e^-$	12.4 ± 0.8
$K_L \to \pi^+\pi^-\pi^0_D$	52.0 ± 7.7
$K_L \to \pi^+\pi^-\pi^0$ with $\pi^0 \to e^+e^-e^+e^-$	10.3 ± 1.1
$K_L \to \pi^+\pi^-\pi^0$ with $\pi^0 \to e^+e^-$	0.6 ± 0.1
$K_S \to \pi^+\pi^-\gamma$ with $\gamma \to e^+e^-$	0.5 ± 0.5
Total	103.0 ± 10.2

Table 2
Background to $K_L \to \pi^+\pi^-\pi^0_D$.

Source	$N^{bkg}_{\pi\pi ee\gamma}$
Collimator scattering	3.7 ± 3.7
Accidental activity	8.0 ± 2.6
$K_S \to \pi^+\pi^-e^+e^-$ + bremsstrahlung	11.6 ± 1.4
$K_S \to \pi^+\pi^-\pi^0_D$	3.7 ± 2.8
$K_L \to \pi^+\pi^-\pi^0$ with $\pi^0 \to e^+e^-e^+e^-$	27.0 ± 1.1
$K_L \to \pi^+\pi^-\pi^0$ with $\gamma \to e^+e^-$	1.1 ± 1.1
Total	55.1 ± 5.7

events was also found to originate from neutral kaons produced or scattered in the collimators (16%). Such events were estimated by extrapolating to the signal region the distribution of $K_S \to \pi^+\pi^-e^+e^-$ candidates located at high $|\vec{r}_{COG}|$ values and in $M_{\pi\pi ee}$ side-band regions. The amount of $K_S \to \pi^+\pi^-\gamma$ events with the photon converting in the *Kevlar* window in front of the spectrometer was found to be small with respect to the total background contribution ($< 1\%$) owing to the strong rejection of such events by the separation requirement between the two electrons in the first drift chamber.

The selection of $K_L \to \pi^+\pi^-\pi^0_D$ events is very similar to the one for the $K_S \to \pi^+\pi^-e^+e^-$. We required, in addition to the four identified charged particles, the presence of an isolated cluster in the LKr calorimeter, within 5 ns of the 4-track event and with an energy greater than 2 GeV, well above the detector noise of 100 MeV per cluster. The distance of the cluster to any dead cell was required to be greater than 2 cm and the distance to any of the four impact points of the charged particles on the LKr to be greater than 15 cm. Candidates were accepted if the reconstructed $e^+e^-\gamma$ invariant mass was in the 110–150 MeV/c^2 range, compatible with the π^0 mass value. The origin of the $K_L \to \pi^+\pi^-\pi^0_D$ was verified in a similar way to the $K_S \to \pi^+\pi^-e^+e^-$ selection, by extrapolating the total momentum vector of the $\pi^+\pi^-e^+e^-\gamma$ state to the final collimator exit face. Moreover, identical analysis cuts as the ones applied to the $K_S \to \pi^+\pi^-e^+e^-$ samples were imposed on the $\pi^+\pi^-e^+e^-\gamma$ final state for $\vec{r}_{COG}$, $p^2_\perp$ and invariant mass variables. However, no lifetime cut was applied in the case of the $K_L \to \pi^+\pi^-\pi^0_D$ decay mode.

After all selection criteria were applied, the total number of $K_L \to \pi^+\pi^-\pi^0_D$ candidates in the 60 to 160 GeV energy range was found to be 58 983 with a background contamination estimated to be smaller than 0.1% (see Table 2). The invariant $M_{\pi\pi ee\gamma}$ mass distribution of events obtained after all other selection criteria were applied is shown in Fig. 1(b).

5. Acceptance

The acceptance for signal and normalization decay channels was computed using a detailed Monte Carlo program based on GEANT3 [10]. Particle interactions in the detector material as well as the response functions of the different detector elements were taken into account in the simulation. In particular, drift chamber resolution functions and wire inefficiencies measured during data taking were introduced at the event reconstruction level. Full shower development in the calorimeters was performed for incident photons, electrons and charged pions to compute energy depositions in the detectors.

Kaon decays in the detector fiducial region were generated using production spectra at the K_S target that were determined from the analysis of the abundant $K_S \to \pi^+\pi^-$ sample and the normalization $K_L \to \pi^+\pi^-\pi^0_D$ channel. The kaon momentum spectrum used for the acceptance calculation ranged between 60 and 160 GeV/c.

The PHOTOS code [11] was implemented in the simulation program to take into account radiative effects in the acceptance calculation for both signal and normalization channels. This algorithm provided the corrections from QED bremsstrahlung in the leading-logarithmic approximation with the proper soft photon behaviour taken into account. A cut-off value of 0.2 MeV in the rest frame of the parent of the radiating charged particle was used for the emitted photon. As a check of the method, the response of the PHOTOS algorithm was compared with the calculations of Isidori [12], valid in the soft-photon approximation. A reasonable agreement was obtained for both $K_S \to \pi^+\pi^-e^+e^-$ and $K_L \to \pi^+\pi^-\pi^0_D$ decay channels when a maximum missing energy of 5 MeV was imposed for the undetected photons. For higher missing energy values, discrepancies between the two computations were observed but these mostly cancelled out in the signal to normalization ratio. We also verified the consistency of the results with existing calculations of radiative corrections [13] in the particular case of the $\pi^0 \to e^+e^-\gamma$ process.

The value of the acceptance depends on the decay matrix element of the process investigated. For $K_S \to \pi^+\pi^-e^+e^-$ decays, the only term considered in the decay amplitude comes from the inner bremsstrahlung process which can be related to the well measured $K_S \to \pi^+\pi^-$ decay rate. For the $K_L \to \pi^+\pi^-\pi^0_D$ channel, we used the current experimental values of the $K_L \to \pi^+\pi^-\pi^0$ decay parameters and of the π^0 electromagnetic form factor [14].

After all selection criteria discussed in the previous section were applied to the reconstructed Monte Carlo events, the average acceptances for $K_S \to \pi^+\pi^-e^+e^-$ and $K_L \to \pi^+\pi^-\pi^0_D$ decays were found to be $(2.804 \pm 0.006)\%$ and $(1.644 \pm 0.002)\%$, respectively. The quoted uncertainties result from the event statistics only. Fig. 2 shows a comparison between data and simulation for the reconstructed kaon longitudinal decay vertex and energy distributions for both signal and normalization events.

6. Branching ratio

The branching ratio of the $K_S \to \pi^+\pi^-e^+e^-$ decay mode was measured relative to $K_L \to \pi^+\pi^-\pi^0_D$ using the following relation:

$$R_{BR} = \frac{BR(K_S \to \pi^+\pi^-e^+e^-)}{BR(K_L \to \pi^+\pi^-\pi^0_D)} = \frac{N_{\pi\pi ee}}{N_{\pi\pi\pi^0_D}} \frac{A_{\pi\pi\pi^0_D}}{A_{\pi\pi ee}} R_\epsilon R_K, \qquad (3)$$

where $N_{\pi\pi ee}$ and $N_{\pi\pi\pi^0_D}$ are, respectively, the signal and normalization yields obtained after background subtraction, $A_{\pi\pi ee}$ and $A_{\pi\pi\pi^0_D}$ are the corresponding acceptances, $R_\epsilon = \epsilon_{\pi\pi\pi^0_D}/\epsilon_{\pi\pi ee}$ is the relative normalization to signal trigger efficiency, and R_K is the ratio, between normalization and signal channels, of the numbers of kaons decaying in the fiducial region. This ratio depends on both the kaon production spectrum and the K_L–K_S lifetime difference. The average value of R_K, over the investigated energy range, was computed to be 0.142.

In order to minimize potential biases due to the energy dependence of the observed yields, acceptances and kaon spectra for

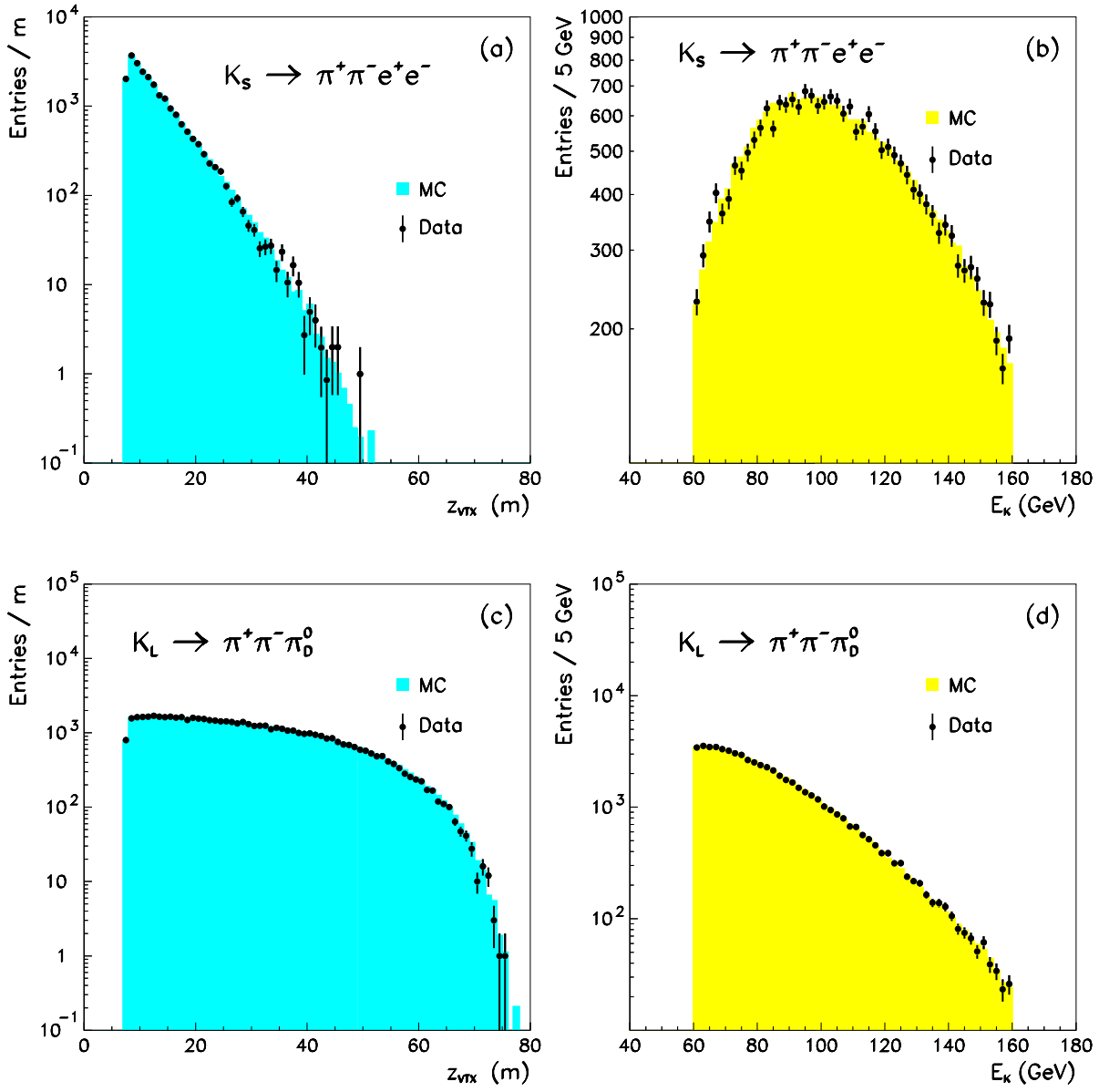

Fig. 2. Longitudinal vertex position (left) and kaon reconstructed energy (right) distributions after background subtraction for $K_S \to \pi^+\pi^-e^+e^-$ (top) and $K_L \to \pi^+\pi^-\pi^0_D$ (bottom) decays, respectively.

both decay channels, data were subdivided in 10 bins, from 60 to 160 GeV, in the reconstructed kaon energy variable and Eq. (3) was computed for each energy bin. The measured $K_S \to \pi^+\pi^-e^+e^-$ branching ratio relative to the $K_L \to \pi^+\pi^-\pi^0_D$ one is shown as a function of the reconstructed kaon energy in Fig. 3. A fit to the data with a constant parameter gave the result:

$$R_{BR} = \frac{BR(K_S \to \pi^+\pi^-e^+e^-)}{BR(K_L \to \pi^+\pi^-\pi^0_D)} = (3.28 \pm 0.06_{stat} \pm 0.04_{syst}) \times 10^{-2} \quad (4)$$

with $\chi^2/ndf = 8.8/9$ when in each energy bin, statistical uncertainties only are taken into account. The statistical error on R_{BR} ratio is dominated by the uncertainty on the trigger efficiency. The latter was found, however, to be rather constant as a function of the kaon energy. After correcting (−0.5%) for possible trigger losses due to high multiplicity events in the drift chambers, we obtained the average value $\langle R_\epsilon \rangle = 1.023 \pm 0.018$ over the 60 to 160 energy range, in agreement with the prediction of 1.016 from the trigger simulation.

The systematic uncertainty quoted in Eq. (4) was estimated from the various contributions presented in Table 3. Since the branching ratio was determined with the hypothesis of a pure inner bremsstrahlung term in the $K_S \to \pi^+\pi^-e^+e^-$ amplitude, the systematic uncertainty due to matrix element parameters was computed only for the normalization channel (0.2%). Contributions from background contaminations (0.1%) and beam parameters (0.1%) were found to be rather small. A conservative estimate of 0.4% on the uncertainty due to radiative corrections was obtained by comparing the branching ratio with and without radiative effects. Contributions due to geometrical (0.7%) and kinematical (0.3%) cuts were computed by estimating possible systematic biases on the result when selection criteria were modified around their nominal values. The largest uncertainties originated from the acceptance radial cuts around the beam pipe in the DCH and LKr detectors and from the two-electron separation in the most up-

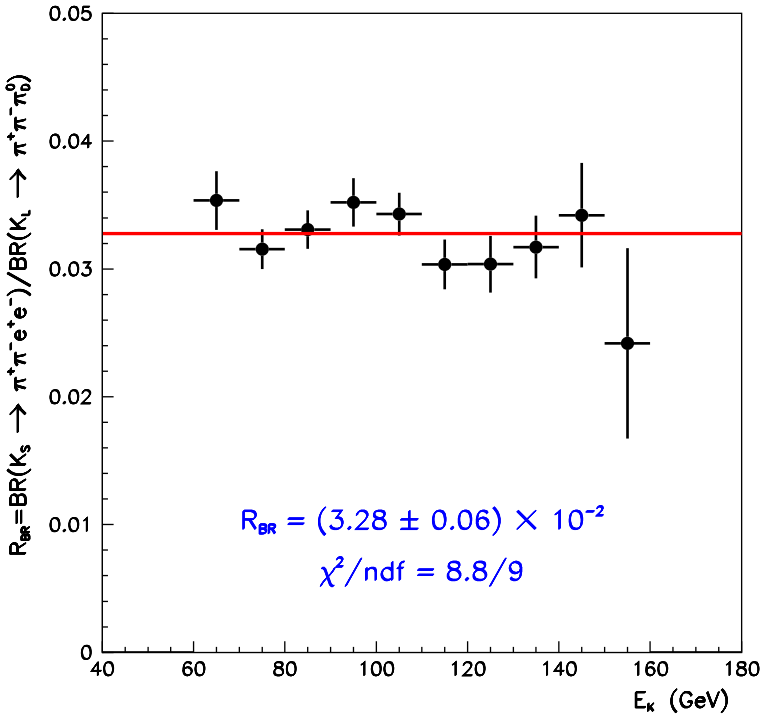

Fig. 3. Measurement of the ratio R_{BR} as a function of the kaon reconstructed energy. Only statistical uncertainties are shown.

Table 3
Systematic uncertainties on R_{BR},

Source	σ_{syst} (%)
$K_L \to \pi^+\pi^-\pi^0$ matrix element	±0.2
Background subtraction	±0.1
Radiative corrections	±0.4
Trigger efficiency	±0.4
e–π separation	±0.2
π decay rejection	±0.6
Beam parameters	±0.1
Geometrical cuts	±0.7
$K_{L,S}$ lifetimes	±0.3
Kinematical cuts	±0.3
Reconstruction	±0.3
Total	±1.2

stream drift chamber. The uncertainty associated to the knowledge of the relative number of K_S and K_L decays in the fiducial decay region was found to be dominated by the experimental errors on the kaon lifetimes (0.3%) [14]. A relative systematic uncertainty of 0.6% was assigned for the rejection of pion decays due to inefficiencies in the muon detector and to the fact that pion decays occurring downstream of the magnetic spectrometer were not included in the simulation. Finally, systematic uncertainties due to the trigger, offline reconstruction and e/π identification were estimated to be 0.4%, 0.3% and 0.2%, respectively.

Summing in quadrature the statistical and systematic uncertainties, we obtained:

$$\frac{BR(K_S \to \pi^+\pi^-e^+e^-)}{BR(K_L \to \pi^+\pi^-\pi^0_D)} = (3.28 \pm 0.07) \times 10^{-2}. \quad (5)$$

This result is in agreement with the measurement of [5] and has a relative precision which is about 2.5 times better. Using the existing values for the $K_L \to \pi^+\pi^-\pi^0$ and $\pi^0 \to e^+e^-\gamma$ branching ratios [14], we found:

$$BR(K_S \to \pi^+\pi^-e^+e^-) = (4.93 \pm 0.14) \times 10^{-5}, \quad (6)$$

where the uncertainty due to the normalization branching ratio is comparable to the statistical one. Our result is in agreement with the published NA48 value [5] of $(4.69 \pm 0.30) \times 10^{-5}$ and can be used to determine the CP-violating inner bremsstrahlung part of the analogous $K_L \to \pi^+\pi^-e^+e^-$ branching ratio through the relation:

$$BR(K_L^{BR} \to \pi^+\pi^-e^+e^-) = \frac{\tau_L}{\tau_S}|\eta_{+-}|^2 BR(K_S \to \pi^+\pi^-e^+e^-). \quad (7)$$

From Eq. (6) and Eq. (7), and using the experimental values for τ_S, τ_L and η_{+-} [14], we found:

$$BR(K_L^{BR} \to \pi^+\pi^-e^+e^-) = (1.41 \pm 0.04) \times 10^{-7}, \quad (8)$$

consistent with the theoretical prediction of 1.3×10^{-7} [1].

7. E1 direct emission

The possibility that the E1 direct emission (CP-even) amplitude gives a contribution to the $K_S \to \pi^+\pi^-e^+e^-$ decay was also investigated. Following Seghal and Wanninger formalism for the radiative $K_S \to \pi^+\pi^-\gamma$ decay [1], the amplitude that governs such a process can be written as:

$$\mathcal{M}_{E1} = e^2 \frac{g_{E1}}{M_K^4} e^{i\delta_1(M^2_{\pi\pi})}\left[(p_- \cdot k)p_{+\mu} - (p_+ \cdot k)p_{-\mu}\right] \times \frac{\bar{u}(k_-)\gamma^\mu v(k_+)}{k^2} \quad (9)$$

where g_{E1} is the parameter that gives the magnitude of E1 direct emission and $\delta_1(M^2_{\pi\pi})$ is the $\pi\pi$ scattering phase in the $I = 1$ p-wave state, evaluated at the energy $M_{\pi\pi}$. Such contribution modifies the energy spectrum E_{γ^*} of the emitted virtual photon in the $K_S \to \pi^+\pi^-\gamma^*$ process as well as the value of the branching ratio. To extract the g_{E1} parameter, a fit to the measured E_{γ^*} spectrum, obtained after background subtraction, was performed by varying

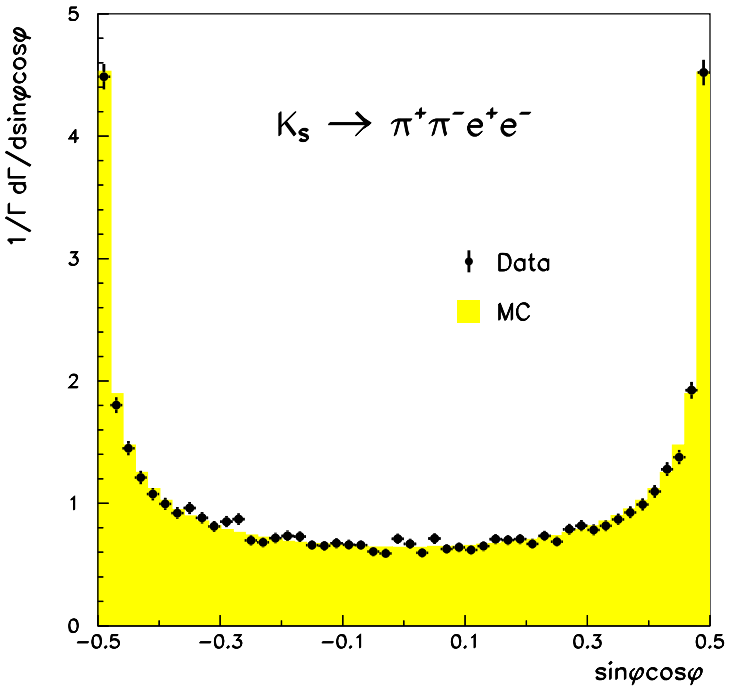

Fig. 4. $K_S \to \pi^+\pi^-e^+e^-$ normalized differential decay rate in the $\sin\phi\cos\phi$ variable.

in the Monte Carlo simulation the contribution of g_{E1} with respect to g_{BR}. The best-fit estimation of g_{E1}/g_{BR} is:

$$\frac{g_{E1}}{g_{BR}} = 1.5 \pm 1.1 \tag{10}$$

with a χ^2/ndf value of 12.8/17. This result is consistent with no observation of E1 direct emission in the $K_S \to \pi^+\pi^-e^+e^-$ decay. After taking into account systematic uncertainties associated to acceptance and kinematical cuts as well as radiative corrections, event reconstruction and π decay rejection, we set the upper limit:

$$\left|\frac{g_{E1}}{g_{BR}}\right| < 3.0 \tag{11}$$

at 90% CL, which corresponds to a contribution from E1 direct emission to the $K_S \to \pi^+\pi^-e^+e^-$ branching ratio of $\pm 0.04 \times 10^{-5}$.

8. Asymmetry measurement

The measurement of the CP-violating asymmetry $\mathcal{A}_\phi$ in $K_S \to \pi^+\pi^-e^+e^-$ decays can be obtained from the distribution of events in the $\sin\phi\cos\phi$ variable:

$$\mathcal{A}_\phi = \frac{N_{\pi\pi ee}(\sin\phi\cos\phi > 0) - N_{\pi\pi ee}(\sin\phi\cos\phi < 0)}{N_{\pi\pi ee}(\sin\phi\cos\phi > 0) + N_{\pi\pi ee}(\sin\phi\cos\phi < 0)} \tag{12}$$

with the quantity $\sin\phi\cos\phi$ defined as:

$$\sin\phi\cos\phi = (\hat{n}_{ee} \times \hat{n}_{\pi\pi}) \cdot \hat{z}(\hat{n}_{ee} \cdot \hat{n}_{\pi\pi}). \tag{13}$$

In Eq. (13), $\hat{n}_{ee}$ and $\hat{n}_{\pi\pi}$ are, respectively, the unit vectors normal to the e^+e^- and $\pi^+\pi^-$ planes, and $\hat{z}$ is the unit vector along the $\pi^+\pi^-$ momentum direction in the kaon centre of mass system. Inspection of Eq. (13) shows that $\sin\phi\cos\phi$ changes sign under CP.

The normalized differential decay rate $(1/\Gamma)(d\Gamma/d\sin\phi\cos\phi)$, obtained after background subtraction and acceptance correction, is shown in Fig. 4. The corresponding asymmetry parameter was found to be consistent with zero:

Table 4
Systematic uncertainties on $\mathcal{A}_\phi$.

Source	$\sigma_{\mathcal{A}_\phi}$ (%)
Radiative corrections	±0.1
Geometrical cuts	±0.3
Kinematical cuts	±0.2
e–π separation	±0.1
Trigger	±0.1
π decay rejection	±0.1
Total	±0.4

$$\mathcal{A}_\phi = (-0.4 \pm 0.7_{stat} \pm 0.4_{syst})\%, \tag{14}$$

where the various contributions to the systematic uncertainty on $\mathcal{A}_\phi$ are given in Table 4.

The largest contribution comes from geometrical cuts on tracks near the beam pipe in the drift chambers and the LKr calorimeter, as well as from the minimum separation between the two electron tracks in the most upstream drift chamber. As far as radiative effects are concerned, the assigned systematic uncertainty was obtained from the comparison between the acceptances obtained using MC runs performed with and without radiative corrections. Contributions from the finite resolution on the ϕ determination were also investigated but were found to be negligible for asymmetry values close to 0.

Summing in quadrature the statistical and systematic uncertainties on $\mathcal{A}_\phi$, we obtained:

$$\mathcal{A}_\phi = (-0.4 \pm 0.8)\%. \tag{15}$$

No evidence for a CP-violating contribution in the $K_S \to \pi^+\pi^-e^+e^-$ decay amplitude was observed. This result was used to set the limit:

$$|\mathcal{A}_\phi| < 1.5\% \tag{16}$$

at 90% CL.

9. Conclusion

Using the NA48/1 data collected in 2002, a precise measurement of the $K_S \to \pi^+\pi^-e^+e^-$ branching ratio relative to the $K_L \to \pi^+\pi^-\pi^0_D$ one was obtained. This result allowed to put an upper limit on a possible E1 direct emission term in the $K_S \to \pi^+\pi^-e^+e^-$ decay amplitude. The CP-violating asymmetry $\mathcal{A}_\phi$ was found to be consistent with zero with a precision five times better than the existing value. The measurements presented in this Letter provide stronger support for a description of the $K_S \to \pi^+\pi^-e^+e^-$ decay amplitude that is dominated by the CP-even inner bremsstrahlung mechanism.

Acknowledgements

It is a pleasure to thank the technical staff of the participating laboratories, universities and affiliated computing centres for their efforts in the construction of the NA48 apparatus, in the operation of the experiment, and in the processing of the data.

References

[1] L.M. Sehgal, M. Wanninger, Phys. Rev. D 46 (1992) 1035;
L.M. Sehgal, M. Wanninger, Phys. Rev. D 46 (1992) 5209, Erratum.
[2] P. Heiliger, L.M. Sehgal, Phys. Rev. D 48 (1993) 4146;
P. Heiliger, L.M. Sehgal, Phys. Rev. D 60 (1999) 079902, Erratum.
[3] A. Alavi-Harati, et al., Phys. Rev. Lett. 84 (2000) 408.
[4] A. Alavi-Harati, et al., Phys. Rev. Lett. 96 (2006) 101801.
[5] A. Lai, et al., Eur. Phys. J. C 30 (2003) 33.
[6] H. Taureg, et al., Phys. Lett. B 65 (1976) 92.
[7] A. Lai, et al., Phys. Lett. B 496 (2000) 137.
[8] V. Fanti, et al., Nucl. Instrum. Methods A 574 (2007) 433.
[9] S. Anvar, et al., Nucl. Instrum. Methods A 419 (1998) 686;
S. Anvar et al., Prepared for IEEE Nuclear Science Symposium (NSS) and Medical Imaging Conference (MIC), Toronto, Ontario, Canada, 8–14 November 1998, DAPNIA-99-06 (1999) 1.
[10] GEANT description and simulation tool, CERN Program Library Long Writeup W5013 (1994) 1.
[11] E. Barberio, B. van Eijk, Z. Wąs, Comput. Phys. Commun. 66 (1991) 115;
E. Barberio, Z. Wąs, CERN-TH 7033/93 (1993) 1.
[12] G. Isidori, Eur. Phys. J. C 53 (2008) 567.
[13] K.O. Mikaelian, J. Smith, Phys. Rev. D 5 (1972) 1763.
[14] Particle Data Group, Phys. Lett. B 667 (2008) 1.